



## Structural, Optical, Photoluminescence Studies onto the Incorporation of Copper in Tin Oxide Nanostructure and Evaluation of their Antimicrobial Property

R. RATHINABALA<sup>1</sup> and R. THAMIZ SELVI<sup>2,\*</sup>

<sup>1</sup>Department of Research and Development, Bharathiar University, Coimbatore-641046, India

<sup>2</sup>Department of Chemistry, Government Arts College (Autonomous), Coimbatore- 641018, India

\*Corresponding author: E-mail: [thamizslv@yahoo.co.in](mailto:thamizslv@yahoo.co.in)

Received: 18 January 2020;

Accepted: 18 March 2020;

Published online: 27 June 2020;

AJC-19922

Biosynthesis of undoped and copper doped tin oxide (SnO<sub>2</sub>) nanoparticles were carried out using *Canna indica* leaf extracts as reducing agents. The as-synthesized nanoparticles were characterized using the powder X-ray diffraction (PXRD), scanning electron microscope (SEM), Fourier transformed infrared spectroscopy (FTIR), UV-visible spectroscopy and photoluminescence (PL). Antimicrobial behaviour of the synthesized nanoparticles was examined. The XRD studies revealed that the rutile structure for both undoped and copper doped SnO<sub>2</sub> nanoparticles, with the absence of secondary phases. The SEM micrographs clearly showed the formation of well-defined spherical particles with no impure phases. The optical absorption studies explained that the variation of band gap with particle size. The photoluminescent spectra showed an emission peaks at 390, 520 and 790 nm, which are ascribed to the structural defects due to the oxygen vacancy. The antibacterial investigation suggested a better antibacterial activity for *Staphylococcus aureus* against *Escherichia coli* bacterial strains.

**Keywords:** Tin oxide nanoparticles, Copper dopant, *Canna indica*, Band gap, Antimicrobial activity.

### INTRODUCTION

Among the nanomaterials, metal and metal oxides gains much interest between the researchers due to its impact in medicinal, electrical, chemical and food industries, *etc.* [1]. Tin oxide (SnO<sub>2</sub>) is one of the deceptive transition metal oxide and it is a *n*-type semiconductor with a band gap 3.6 eV [2]. Rutile structure of SnO<sub>2</sub> nanoparticles possessing various applications such as photo catalysis, oxidative catalysis, dye sensitized cell, optoelectronic devices, conductive glasses, thermal, gas sensing, *etc.* [3,4]. Furthermore, the assessment of antimicrobial activity of tin oxide nanoparticles has become an important application in pharmacological science [5]. An antibacterial agent attains abundant attention in many fields like medicine, sanatorium and food disinfection [6,7]. Tin oxide nanoparticles are well playing a vital role in scavenging these toxic free radicals thereby terminating the oxidative damage of human body.

In order to stimulate the physio-chemical and biological performance of metal oxide nanoparticles, it is often doped with other metals like copper, cobalt, chromium, magnesium,

cadmium, iron, antimony and indium to incorporate donor sites near to the conduction band making the host material as an *n*-type semiconductor [8]. These dopants improved the surface and stimulate the performance of host material by inducing decrement in size as well as modification in its shapes [9].

The synthesis of nanomaterials can be carried out using various techniques, which include microwave [10], sol-gel [11], hydrothermal [12] and chemical co-precipitation [13-17], *etc.* From the earlier reports, it is understood that the synthesis of nanoparticles are associated with the addition of large amount of toxic chemicals, low product efficiency, non-economical and formation of nano-pollutants which are difficult to destroy. In this perception, Greener approach gains interest of many chemists, biologists and material scientists to discover eco-friendly methods [18,19]. It is cost effective, biocompatible, less toxic and consequently can be used as a significant substitute. In chemical methods of nanoparticles synthesis, the stability of product may depend on the reducing and capping agents [20] but in greener methods, presence of various bioactive components like terpenoids, fixed oils, alkaloids, phenolic compounds,

glycosides, tannins, saponins, flavonoids, amino acids, fatty acids and carbohydrates in the parts of plant components are acted as reducing, stabilizing and capping agents. These are mainly used to synthesize, metal oxide nanoparticles with controlled particle size [21], morphology, physio-chemical behaviours [22] and reactivity [23].

In the present study, biosynthesis of undoped and copper doped SnO<sub>2</sub> nanoparticles with variable mole percentage concentrations were done using *Canna indica* leaf extracts as reducing agent. The synthesized nanoparticles were subjected to XRD, SEM, FT-IR, UV and photoluminescence studies. Antibacterial analyses were also done for evaluation of their biological benefits.

## EXPERIMENTAL

Tin(II) chloride dihydrate, copper sulphate pentahydrate, were procured from Merck (India). The chemicals used in this study were of analytical grade and used as such without any more purification process. Fresh green leaves of *Canna indica* plant were collected from the Nallur village in Tirupur district, of India.

**Preparation of *Canna indica* leaf extract:** Collected *Canna indica* leaves were washed many times with deionized water to remove dust, sand and any other impurities present in it. It was then dried, cut into finer pieces, weighed for 50 mg and kept in boiling water for a period of 10 min in a 250 mL Erlenmeyer flask. The colour of the aqueous solution changed dirty white. It was then filtered using Whatman filter No.1 and centrifuged at 1200 rpm for a period of 5 min to remove the heavier biomaterials.

**Synthesis of undoped and copper doped tin oxide nanoparticles:** Undoped SnO<sub>2</sub> nanoparticles were prepared via greener route method with the help of *Canna indica* leaves extracts. Exactly, 90 mL of 1 mM tin chloride solution was taken in a 250 mL round bottom flask and kept under magnetic stirring at 70 °C. To this 10 mL of *Canna indica* leaf extract were added dropwise and the precipitate formation was noticed. This indicates the completion of the reaction with the formation of tin oxide nanoparticles. The product obtained was filtered, and washed several times with deionized water to remove the residual chloride ions, if any present in the sample. Further washing the pot using ethanol to ensure the purity of product formed. Finally, the product was dried in vacuum oven overnight at 60 °C.

Similar procedure was adopted for synthesis of 1-3 mol% of copper doped SnO<sub>2</sub> nanoparticles by the addition of corresponding mol% solution of copper sulphate pentahydrate to the tin(II) chloride dihydrate solution.

**Antimicrobial activity:** Antimicrobial potential of green synthesized SnO<sub>2</sub> nanoparticles and copper doped SnO<sub>2</sub> nanoparticles was tested by well-diffusion assay. Muller-Hinton agar plates inoculated log phasic culture and wells were created using 50 mm stainless sterile well puncture. Undoped (50 µL) and copper doped SnO<sub>2</sub> nanoparticles containing final concentration of 25, 50 and 75 µg mL<sup>-1</sup> were studied against pathogenic Gram-positive and negative bacterial strains. The plates

were hatched at 30 °C for 24 h and the results were noted by evaluating the zone of inhibition.

**Characterizations:** The X-ray diffraction patterns of the samples were obtained on Bruker AXS D8-Advanced X-ray diffractometer using CuKα radiation at 2θ values between 20° and 80°. Model Jeol JSM-6390 microscope operating at 20 kV equipped with EDAX attachments was used to study the surface morphology and the elemental compositions of undoped and copper doped tin oxide nanoparticles, respectively. The FT-IR of undoped and copper doped tin oxide nanoparticles were recorded with the help of Bruker-Tensor, in the range from 4000 to 400 cm<sup>-1</sup> to study the presence of the functional groups. The optical absorption analysis of the nano particles was done by ultraviolet-visible (UV-Vis) Spectrometer (Jasco-16393). The photoluminescence spectra (PL) analyses were done by using Perkin-Elmer LS 45.

## RESULTS AND DISCUSSION

**XRD analysis:** Fig. 1 shows the XRD pattern of undoped SnO<sub>2</sub> and copper doped SnO<sub>2</sub> nanoparticles (1-3 mol%). The diffraction peaks consistent to (110), (101), (211) and (310) planes were found to reveal the tetragonal rutile structure in position and relative intensity (JCPDS Card No. 41-1445) for both undoped and copper doped samples. The broadness of the peaks indicates the formation of nanoparticles with lower crystalline nature. The rutile structure is conserved and no impurity phases were noted. This may be due to the homogenization of copper onto tin oxide lattice. The average crystallite size of as prepared samples was calculated using the Debye-Scherrer's equation:

$$D = \frac{k\lambda}{\beta \cos \theta} \quad (1)$$

where D is the grain size, k is a constant taken to be 0.9, λ is the wavelength of X-ray radiation, β is the full width at half maximum (FWHM), θ is the angle of diffraction and (hkl) is the plane values. The calculated average particle size using Debye-Scherrer equation was found to be around 4-5 nm and the surface area was found to be around 188.17 m<sup>2</sup>/g. It was further observed that the diffraction peaks corresponding to increased dopant concentration (2 mol%) shows a slight shift in peak position to higher angle in comparison with undoped SnO<sub>2</sub> nanoparticles. However, with further increase in dopant concentration (3 mol%), the diffraction peaks exhibited slight shift in peak position to lower angle. The contraction in the system may be assigned to the defect related vacancies of tin or oxygen.

**SEM with EDS analysis:** The morphology of the samples were analyzed using the SEM micrographs given in Fig. 2a-d. The micrographs of undoped and copper doped samples exhibited a nearly spherical shape with some agglomerates. The energy dispersive spectral analysis of undoped and 2 mol% copper doped SnO<sub>2</sub> nanoparticles were carried out to ascertain the purity of the as-prepared samples and presented in Fig. 2e-f. The peaks corresponding to Sn, O were noticed for undoped and Sn, O and Cu for doped samples, respectively. No impurity

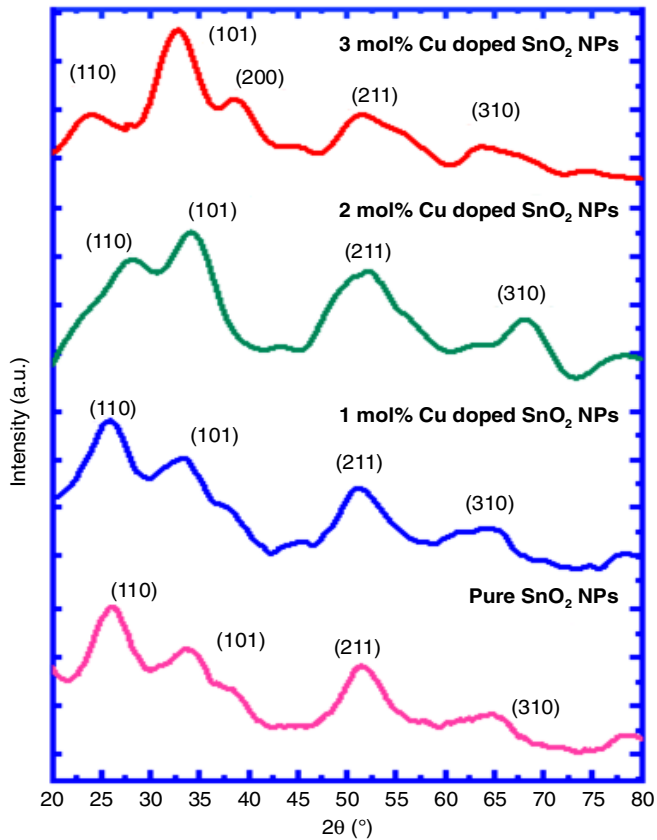


Fig. 1. XRD pattern for un-doped and 1-3 mol% Cu doped SnO<sub>2</sub> NPs

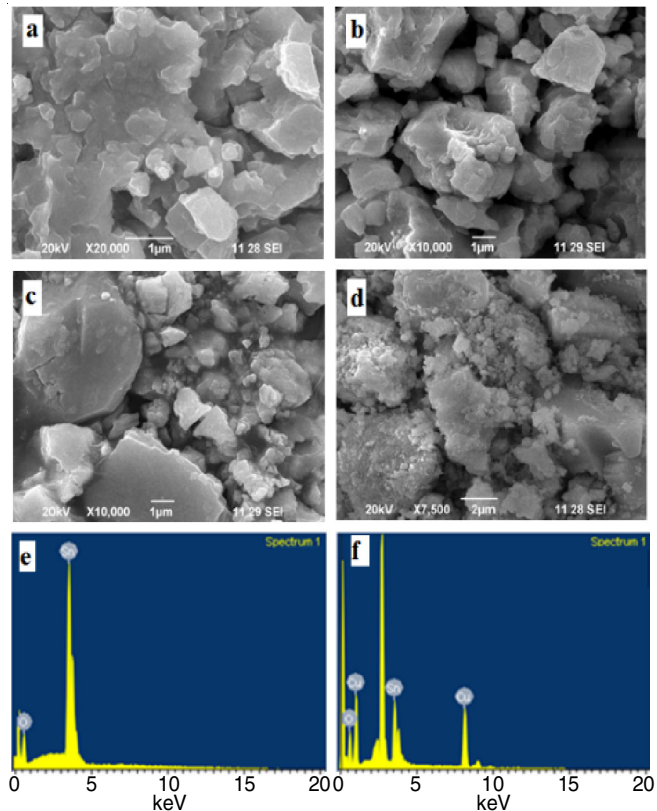


Fig. 2. SEM micrograph of (a) undoped SnO<sub>2</sub>-NPs, (b) 1 mole% Cu doped SnO<sub>2</sub>-NPs, (c) 2 mole% Cu doped SnO<sub>2</sub>-NPs, (d) 3 mole% Cu doped SnO<sub>2</sub>-NPs, (e) EDX spectrum of undoped SnO<sub>2</sub> NPs, (f) EDX spectrum of 2 mole% Cu doped SnO<sub>2</sub> NPs

peaks were observed indicating the purity of the as-prepared samples.

**FTIR analysis:** FT-IR spectra for undoped and copper doped SnO<sub>2</sub> nanoparticles are shown in Fig. 3. A broad absorption band around 3400-3300 cm<sup>-1</sup> representing the presence of hydroxyl group confirmed the moisture content of the samples. This was further evidenced by the formation of hydroxyl group of structural water at 1620 cm<sup>-1</sup>. No significant peak shifts were noticed in undoped and copper doped SnO<sub>2</sub> nanoparticles. The peaks obtained between 700-500 cm<sup>-1</sup> indicate the presence of Sn-O-Sn functional groups. The peak appearing at 571 cm<sup>-1</sup> is a typical vibration of the Sn-O bond in tin oxide [24,25].

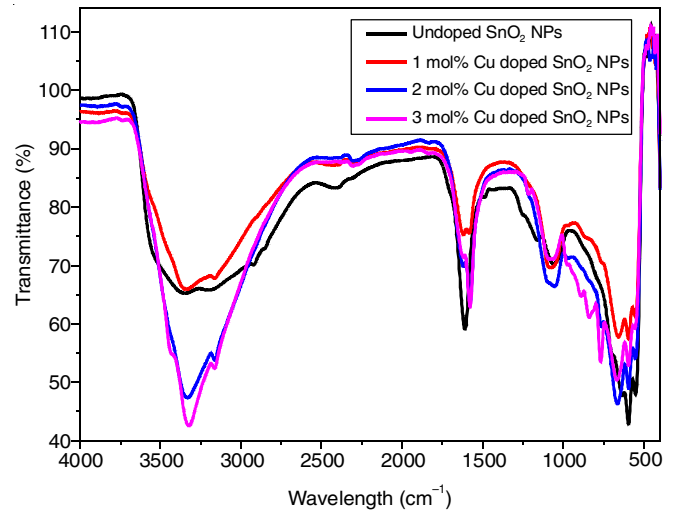


Fig. 3. FTIR spectra of un-doped and 1-3 mol% Cu doped SnO<sub>2</sub>-NPs

**Optical studies:** The UV-visible absorption spectra for the wavelength range of 200 to 900 nm for the undoped and copper doped tin oxide nanoparticles are presented in Fig. 4. A sharp absorption peak at 300 nm and a slightly broad peak at 470 nm were noticed for tin oxide nanoparticles. From Fig. 4, it is evident that the intensity of the absorption peak was found to increase with the increase in dopant concentration (1 and 3

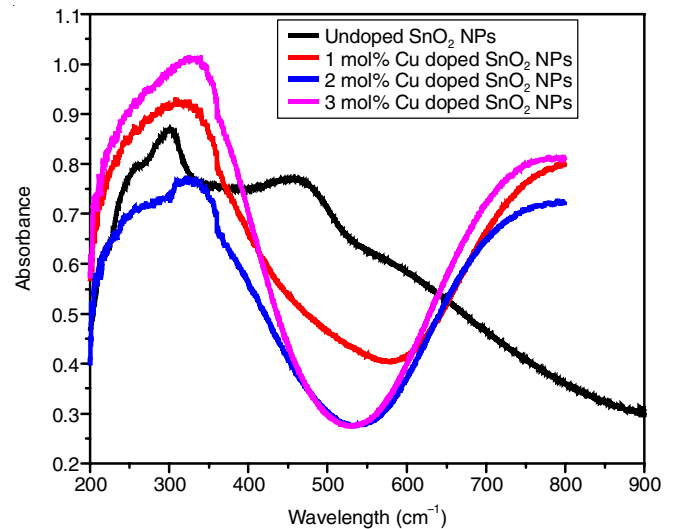


Fig. 4. Absorption spectra of un-doped and 1-3 mol% Cu doped SnO<sub>2</sub> NPs

mol%). This might be due to the size of nanoparticle and defects inside the samples. The absorbance edge was shifted towards longer wavelength for copper doped samples. This may be due to the less strain observed in copper doped samples.

The optical band gap ( $E_g$ ) for undoped and copper doped SnO<sub>2</sub> nanoparticles semiconductor can be obtained from the absorption coefficient ( $\alpha$ ) and photon energy ( $h\nu$ ) by the following equation:

$$\alpha = \frac{A(h\nu - E_g)^{1/2}}{h\nu} \quad (2)$$

where  $E_g$  is the optical band gap of nanoparticles and  $A$  is a constant [26]. A graphical plot of  $(\alpha h\nu)^2$  versus  $h\nu$  is shown in Fig. 5. The intercept gives the value of band gap energy ( $E_g$ ). The band gap for undoped SnO<sub>2</sub> nanoparticles was found to be 3.95 eV and this is higher than the band gap value for bulk SnO<sub>2</sub> nanoparticles (3.6 eV) [27]. Generally, in semiconductors, the band gap is found to be size dependent. The smaller size of the nanoparticles formed in the present study is expected to increase the band gap. However, the decreased band gap (3.8 eV) for 1 mol% of copper doped SnO<sub>2</sub> nanoparticles, may be due to the slight increase in the particle size because of the substitution of copper in tin sites. The more addition of copper (> 1%) exhibited a shift of  $E_g$  from 3.8 to 4.2 eV and then 4.1 eV, respectively. This may be due to electron interactions of *sp* and *d*-orbitals and the substitution of copper in tin sites [28]. The variations in  $E_g$  values may be due to the variation in the particle size.

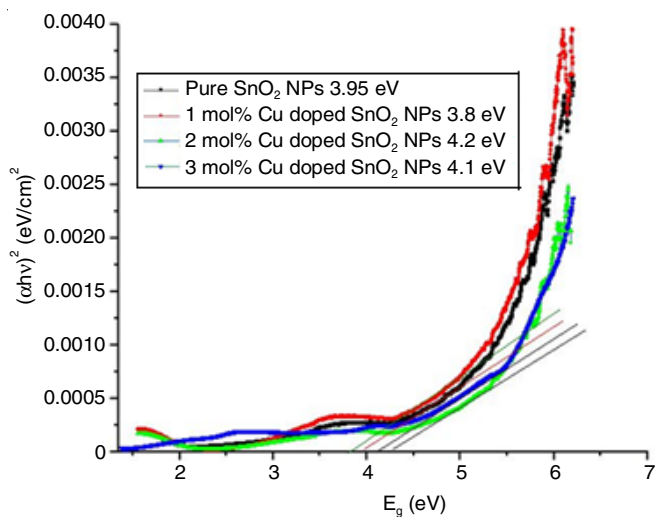


Fig. 5. Band gap energy ( $E_g$ ) of un-doped and Cu doped SnO<sub>2</sub> NPs

**Photoluminescence analysis:** The photoluminescence spectra of undoped and copper doped (1, 2 and 3 mol%) tin oxide nanoparticles were noted at room temperature (Fig. 6) with an excitation wavelength of 300 nm. There is no major shift in the peaks in the UV-visible region, but however the intensities were found to vary. This might be ascribed to the variation in particle size of the as-prepared samples. As the energy of excitation and emission are lower than the band gap of tin oxide, direct recombination of the 4p band of Sn and 2p band of oxygen is not possible. The spectrum shows three emission

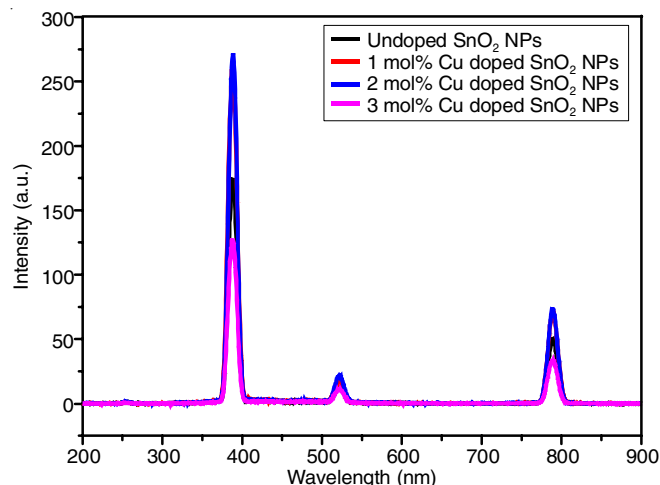


Fig. 6. Photoluminescence spectra of un-doped and 1-3 mol% Cu doped SnO<sub>2</sub> NPs

peaks *viz.* (a) an exciton emission at 390 nm was due to the strong blue emission, (b) a weak green emission at 520 nm is attributed due to oxygen present in the interstitial sites, and (c) peak with a moderate intensity in the red region (790 nm), which may be due to different luminescent centers like oxygen vacancy and the deep level interstitial defects. Pagnier *et al.* [29] reported that the intensity of peak decrement confirmed the formation of bonding between dopant metal and host metal solid solution. In the present case, a decrease of intensity for 3 mol% copper of near band edge emission may be due to the interaction between the doped copper element and tin oxide, which is reflected in the reduction of peak intensity. This might be due to the concentration quenching effect due to the exchange between dopant ions. The results suggested that as-synthesized nanomaterials may find applications for display purposes in optoelectronic devices.

**Antimicrobial activity:** Antimicrobial testing on most common and venerable bacterial pathogens *E. coli* and *S. aureus* showed positive was tested by well-diffusion assay. The bacterial growth was inhibited by SnO<sub>2</sub> nanoparticles. The doping of SnO<sub>2</sub> with 1 mol% copper reflects a variation in the bacterial growth inhibition in both Gram positive and negative bacteria. Bacterial growth inhibitions were found increasing with the concentration of copper doping percentage. Comparison of bacterial growth inhibition was found maximum with *S. aureus* than *E. coli*, which indicated that the membrane diversification among the bacterial species as shown in Fig. 7. Greener synthesized nanoparticles possessed superior antimicrobial activity due to their lower size of nanoparticles and morphology structure like spherical, which can easily attached with the surface of the bacterial plasma membrane, cell walls, proteins and DNA [30]. From the results, it is inferred that the greener synthesized nanoparticles has shown better antibacterial activity against *S. aureus* than *E. coli* bacterial strains.

## Conclusion

Undoped and copper doped tin oxide nanoparticles were synthesized effectively by green route method. X-ray diffraction studies revealed the formation of tetragonal crystal

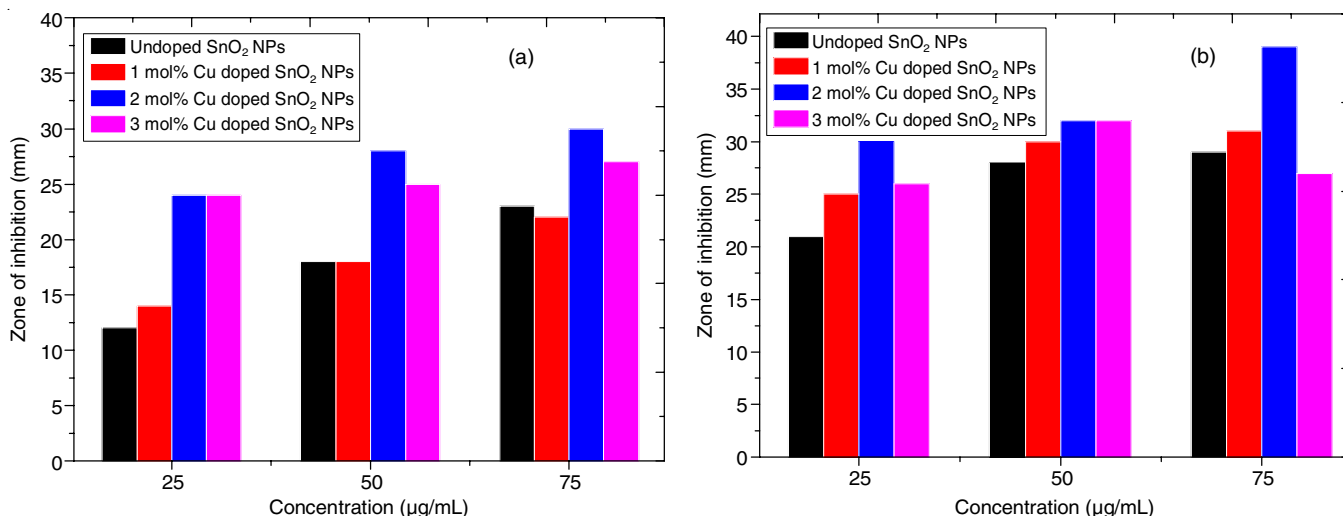


Fig. 7. Comparison of antibacterial susceptibility of un-doped and 1-3 mole% Cu doped SnO<sub>2</sub> NPs against (a) Gram-negative *E. coli* and (b) Gram-positive *S. aureus*

structure for tin oxide. There is no significant change in the average crystallite size by the addition of copper dopant and the diffraction peaks corresponding to secondary phases were absent. The scanning electron micrographs clearly showed the formation of quite spherical nanoparticles and the FTIR spectra revealed the absorption peaks between 640 and 430 cm<sup>-1</sup> of SnO<sub>2</sub> due to the metal-oxygen bond. The optical band gap values of undoped and copper doped SnO<sub>2</sub> nanoparticles were found to vary between 3.8 to 4.2 eV, respectively, in comparison with bulk SnO<sub>2</sub> (3.6 eV). The variation in the photoluminescence intensity emission peaks at 390, 520 and 790 nm confirmed the changes in terms of stoichiometry due to its structural defect. It attributes the successful incorporation of copper in host system. The antibacterial investigation suggested an efficient antibacterial activity against *S. aureus* than *E. coli* bacterial strains.

#### CONFLICT OF INTEREST

The authors declare that there is no conflict of interests regarding the publication of this article.

#### REFERENCES

- M. Gratzel, *Nature*, **414**, 338 (2001); <https://doi.org/10.1038/35104607>
- T. Hyodo, S. Abe, Y. Shimizu and M. Egashira, *Sens. Actuators B Chem.*, **93**, 590 (2003); [https://doi.org/10.1016/S0925-4005\(03\)00208-9](https://doi.org/10.1016/S0925-4005(03)00208-9)
- F. Li, J. Xu, X. Yu, L. Chen, J. Zhu, Z. Yang and X. Xin, *Sens. Actuators B Chem.*, **81**, 165 (2002); [https://doi.org/10.1016/S0925-4005\(01\)00947-9](https://doi.org/10.1016/S0925-4005(01)00947-9)
- A. Corma, L.T. Nemeth, M. Renz and S. Valencia, *Nature*, **412**, 423 (2001); <https://doi.org/10.1038/35086546>
- O. Yamamoto, *Int. J. Inorg. Mater.*, **3**, 643 (2001); [https://doi.org/10.1016/S1466-6049\(01\)00197-0](https://doi.org/10.1016/S1466-6049(01)00197-0)
- Q. Li, S. Mahendra, D.Y. Lyon, L. Brunet, M.V. Liga, D. Li and P.J.J. Alvarez, *Water Res.*, **42**, 4591 (2008); <https://doi.org/10.1016/j.watres.2008.08.015>
- J.M.C. Gutteridge, D.A. Rowley and B. Halliwell, *Biochem. J.*, **199**, 263 (1981); <https://doi.org/10.1042/bj1990263>
- A.K. Sinha, M. Pradhan, S. Sarkar and T. Pal, *Environ. Sci. Technol.*, **47**, 2339 (2013); <https://doi.org/10.1021/es303413g>
- A.A. Zhukova, M.N. Rumyantseva, V.B. Zaytsev, A.V. Zaytseva, A.M. Abakumov and A.M. Gaskov, *J. Alloys Compd.*, **565**, 6 (2013); <https://doi.org/10.1016/j.jallcom.2013.02.184>
- T. Krishnakumar, R. Jayaprakash, N. Pinna, V.N. Singh, B.R. Mehta and A.R. Phani, *Mater. Lett.*, **63**, 242 (2009); <https://doi.org/10.1016/j.matlet.2008.10.008>
- A.A. Firooz, A.R. Mahjoub and A.A. Khodadadi, *Mater. Lett.*, **62**, 1789 (2008); <https://doi.org/10.1016/j.matlet.2007.10.004>
- H.S. Devi, A.H. Sofi, T.D. Singh and M.A. Shah, *J. Nanosci. Nanotechnol.*, **19**, 7707 (2019); <https://doi.org/10.1166/jnn.2019.16844>
- K. Anandan and V. Rajendran, *Superlatt. Microstruct.*, **85**, 185 (2015); <https://doi.org/10.1016/j.spmi.2015.05.031>
- G. Vijayaprasath, R. Murugan, S. Asaithambi, P. Sakthivel, T. Mahalingam, Y. Hayakawa and G. Ravi, *Ceram. Int.*, **42**, 2836 (2016); <https://doi.org/10.1016/j.ceramint.2015.11.019>
- L. Korosi, S. Papp, V. Meynen, P. Cool, E.F. Vansant and I. Dekany, *Colloids Surf. A Physicochem. Eng. Asp.*, **268**, 147 (2005); <https://doi.org/10.1016/j.colsurfa.2005.05.074>
- M.V. Arularasu, M. Anbarasu, S. Poovaragan, R. Sundaram, F.T. Thema, K. Kanimozhi, C.M. Magdalane, K. Kaviyarasu, D. Letsholathebe, G.T. Mola and M. Maaza, *J. Nanosci. Nanotechnol.*, **18**, 3511 (2018); <https://doi.org/10.1166/jnn.2018.14658>
- K. Kaviyarasu, E. Manikandan, J. Kennedy, R. Ladhumananandasiyam, U.U. Gomes, M. Maaza and G.T. Mola, eds.: Y. Oral and Z.B.B. Oral, Improved Photon Conversion Efficiency of SnO<sub>2</sub> Doped Cesium Oxide Nanofibers for Photocatalytic Application Under Solar Irradiation, 3rd International Multidisciplinary Microscopy and Microanalysis Congress (InterM), Springer Proceedings in Physics, vol. 186, p. 113 (2017).
- S.R. Bonde, D.P. Rathod, A.P. Ingle, R.B. Ade, A.K. Gade and M.K. Rai, *Nanosci. Methods*, **1**, 25 (2012); <https://doi.org/10.1080/17458080.2010.529172>
- K.S. Kavitha, S. Baker, D. Rakshith, H.U. Kavitha, B.P. Harini and S. Satish, *Int. Res. J. Biol. Sci.*, **2**, 66 (2013).
- P. Boomi, G. Poorani, S. Palanisamy, S. Selvam, G. Ramanathan, S. Ravikumar, H. Barabadi, H.G. Prabu, J. Jeyakanthan and M. Saravanan, *J. Cluster Sci.*, **30**, 715 (2019); <https://doi.org/10.1007/s10876-019-01530-x>
- K.G. Severin and T.M. Abdel-Fattah, *Chem. Commun.*, **14**, 1471 (1998); <https://doi.org/10.1039/a709067f>

22. I. Nekoksova, N. Ilkova, A. Zukal and J. Cejka, *Stud. Surf. Sci. Catal.*, **156**, 779 (2005);  
[https://doi.org/10.1016/S0167-2991\(05\)80286-1](https://doi.org/10.1016/S0167-2991(05)80286-1)
23. F.-T.J. Ngenefeme, N.J. Eko, Y.D. Mbom, N.D. Tantoh and K.W.M. Rui, *Open J. Compos. Mater.*, **3**, 30 (2013);  
<https://doi.org/10.4236/ojcm.2013.32005>
24. H. Zuoli, Q. Wenxiu, X. Haixia, C. Jing, Y. Yuan and S. Peng, *The Am. J. Ceram. Soc.*, **95**, 3941 (2012);  
<https://doi.org/10.1111/j.1551-2916.2012.05426.x>
25. R. Sangeetha, S. Muthukumaran and M. Ashokkumar, *Spectrochim. Acta A Mol. Biomol. Spectrosc.*, **144**, 1 (2015);  
<https://doi.org/10.1016/j.saa.2015.02.056>
26. X.G. Chen, W.W. Li, J.D. Wu, J. Sun, K. Jiang, Z.G. Hu and J.H. Chu, *Mater. Res. Bull.*, **47**, 111 (2012);  
<https://doi.org/10.1016/j.materresbull.2011.09.019>
27. S. Snega, K. Ravichandran, N. Jabena Begum and K. Thirumurugan, *J. Mater. Sci. Mater. Electron.*, **24**, 135 (2013);  
<https://doi.org/10.1007/s10854-012-0956-6>
28. Y.N. Tan, C.L. Wong, A.R. Mohamed, *Int. Schol. Res. Notices*, **2011**, 261219 (2011);  
<https://doi.org/10.5402/2011/261219>
29. T. Pagnier, M. Boulova, A. Galerie, A. Gaskov and G. Lucazeau, *Sens. Actuators B Chem.*, **71**, 134 (2000);  
[https://doi.org/10.1016/S0925-4005\(00\)00598-0](https://doi.org/10.1016/S0925-4005(00)00598-0)
30. M. Anandan, G. Poorani, P. Boomi, K. Varunkumar, A.A. Chuturgoon, K. Anand, M. Saravanan and H.G. Prabu, *Process Biochem.*, **80**, 80 (2019);  
<https://doi.org/10.1016/j.procbio.2019.02.014>